The interaction of a sodium atom with the silicon(111) surface

M Mahapatra†, A K Ray† and A S Hira‡

† PO Box 19059, Physics Department, University of Texas at Arlington, Arlington, TX 76019, USA
‡ Jarvis Christian College, Hawkins, TX 75765, USA

Abstract. The interaction of a sodium atom with the silicon(111) surface is studied from the point of view of molecular orbital theory. The Si surface is modelled by finite clusters and the interaction of the alkali atom is investigated from different approach positions. Electron correlation is incorporated by invoking the concepts of fourth-order many-body perturbation theory. The results are compared with available data in the literature.

1. Introduction

The interaction of alkali-metal (AM) atoms with silicon clusters is an important field of study from the point of view of gaining an understanding of the electronic properties of metal–semiconductor (MS) junctions [1–5]. In addition to the purely scientific motivation for such studies, the theoretical and experimental knowledge gained from such investigations are expected to be useful in the elucidation and formulation of increasingly complex and versatile device concepts. Potential applications of technological interest include negative electron-affinity (NEA) devices [1], optoelectronics, image intensifiers, Schottky diodes [2], infrared detectors, very-large-scale integrated (VLSI) circuits [3] and spin-polarized electron-beam sources [4]. In this paper, we use Si_n clusters ($n = 2$–10) to model the Si(111) surface and its interactions with Na, with a view to understanding the mechanisms involved in the crystalline evolution, the possible reconstruction of this surface and Si interactions with metal adsorbate. We first present a summary of the relevant work available in the literature.

The experimental work of Avci [6] on Si(111) (7×7) shows that at low coverage ($\leqslant$ 0.3 ML) the alkali atoms (Na, K, Cs and Rb) transfer their s electrons to the Si surface and remain as screened positive centres. For higher coverage (0.3–1.0 ML), the formation of a metallic layer takes place. Papageorgopoulos and Kamaratos [7] have studied experimentally the deposition of Na on (1×1) and (7×7) structures of Si(111). From work-function measurements, they found that the dipole moment of the Na on the (1×1) structure was greater than that on the (7×7) structure. They concluded that this might be due to the facts that the (1×1) structure is more uniform than the reconstructed (7×7) structure and that the average dipole length of Na on the (1×1) structure is greater. Their results from thermal desorption spectra of Na on the Si(111) surface indicate metallization of the Na layer at high coverage and higher binding energy of Na on a reconstructed (7×7) Si surface than on the (1×1) surface.

As far as theoretical work is concerned, Northrup [8] performed a first-principles pseudo-potential calculation within the local-density approximation. His results give a detailed picture of how bonding occurs between Na and Si(111) surface. He considered three

possible adsorption geometries: the onefold top site (OTS), the threefold hollow site (THS) and the threefold filled site (TFS). He concluded that the THS was slightly favoured with respect to the TFS, while the OTS geometry was ruled out for adsorption. In addition the bonding was found to be ionic, formed by the Na 3s orbitals and the dangling-bond orbitals on the Si surface. The Na–Si bond length was found to be 2.71 Å and the ionization potential for Si(111) (1×1):Na was calculated to be 2.1 eV, as compared to 4.8 eV for the ideal surface. Ossicini *et al* [9] studied the interface formed by one monolayer of Na adsorbed on the ideal Si(111) surface by using linear muffin-tin orbital methods in the atomic-sphere approximation. The interaction between Na and the Si surface was found to have both covalent and ionic character, but the covalent one was dominant, with bonding and antibonding structures forming a couple of states around the Si gap. The system formed in this way has a non-metallic character as observed by Northrup [8] and also suggested by Batra and Ciraci [10] on the basis of a study on the K–Si(111) system. The results again preferred the THS, with a charge transfer of $0.29e$.

As indicated above, controversies exist in the studies of AM-atom interactions with the Si(111) surface. The difference in the theoretical results is particularly surprising, since these have mostly used the local-density approximation. In this work, we extend our previous calculations [11–13] and use the techniques of *ab initio* unrestricted Hartree–Fock (UHF) theory [14, 15] to study the interaction of an Na atom with the Si(111) surface. Effects of electron correlation [16–19] are investigated by invoking the concepts of many body perturbation theory (MBPT) at the fourth order level (MP4). All the computations were carried out using the programs GAMESS [20] and GAUSSIAN 92 [21].

2. Bare Si clusters

We have investigated twenty-seven Si clusters in the ideal FCC (111) symmetry. The most stable clusters only are shown in figure 1. In the notation used to represent the Si clusters in this paper, the first number represents the Si atoms taken from the first plane, the second number is for the Si atoms from the second plane and so on. As shown in the figure we have considered both planar and non-planar clusters: ten planar clusters, twelve two-layer clusters, three three-layer clusters and two four-layer clusters. In figure 1 the open circles are the atoms in the first layer and the shaded circles represent the atoms in second layer. The wide range of clusters considered allows for the investigation of physical and chemical properties as functions of cluster size and geometry and also of possible evolutions to bulk properties. For each cluster the total cluster energy was optimized with respect to the interatomic distances or the so-called 'lattice constant', while the interatomic angles were kept fixed at bulk values to preserve the FCC symmetry. Possibilities of different spin states were also investigated. The optimum lattice constant for a given cluster was then used to calculate the fourth-order perturbation-theory energy eigenvalues. The binding energy per atom for a given cluster was then obtained from the formula

$$E_b(\mathrm{Si}_n) = [nE(\mathrm{Si}_1) - E(\mathrm{Si}_n)]/n \tag{1}$$

where $E(\mathrm{Si}_1)$ is the energy of a single Si atom and $E(\mathrm{Si}_n)$ is the energy of an Si cluster with n atoms.

Table 1 lists the optimum lattice constants, the ground-state configurations, the UHF and MBPT ground-state energies and the MBPT binding energies per atom of the Si clusters. Figure 2 shows the binding energy per atom as a function of cluster size. Some odd–even
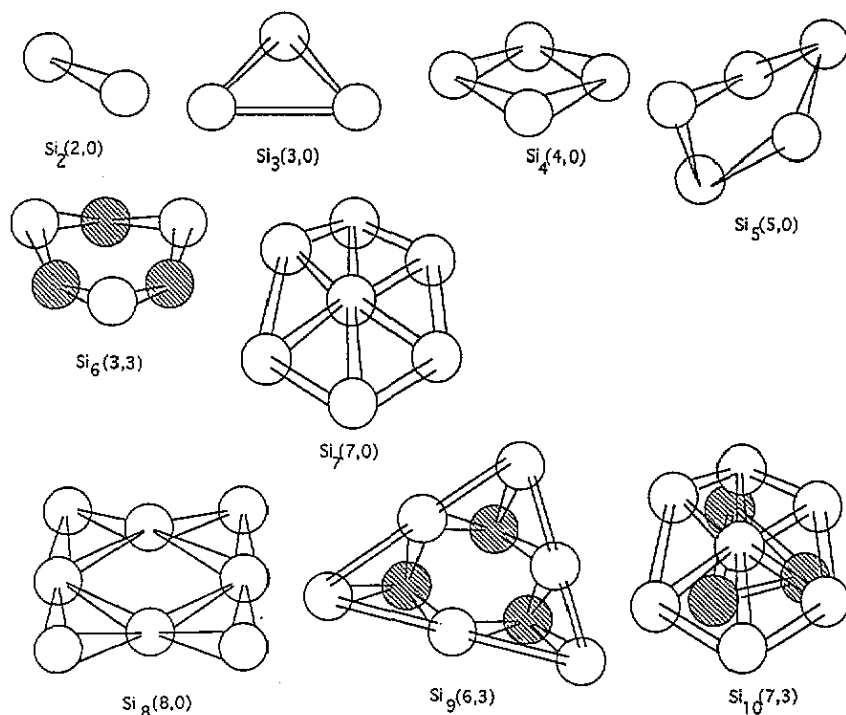
Figure 1. Most stable Si_n clusters in ideal FCC(111) symmetry.

alterations are noted and all the clusters are found to be bound at all levels of theory. The MBPT values of the binding energy per atom range from a minimum of 0.98 eV for $Si_2(2,0)$ to a maximum of 2.12 eV for $Si_8(8,0)$. Thus a maximum of 45.8% of the bulk cohesive energy of 4.63 eV [22] is recovered in the present calculations. We find that even clusters are particularly stable, in partial agreement with the results for free clusters [23–25] and experimental results obtained from mass spectral distribution [26–30] and photofragmentation [26]. Also, the singlet states are more stable than the triplet states as found in some previous theoretical studies [23–25] on Si clusters. To compare with some other works in the literature, for the Si_2 molecule, our calculated electronic state $^3\Sigma_g$ is in agreement with experiment [31] and the error in our bond length of 2.285 Å is only 1.7% compared to the experimental bond length of 2.246 Å. For Si_4, the D_{2h} ^1A_g rhombic structure is found to be the most stable structure. This agrees with some previous calculations [23–25], but disagrees with the results of semiempirical calculations on Si_4 [32, 33]. It can be noted that, in general, the planar clusters are more stable than the clusters with two layers and that cluster stability decreases with increasing number of layers for $n \leqslant 8$. For larger clusters (n > 8), one notices an increase in cluster stability by the addition of third and fourth layer atoms. As far as lattice constant is concerned, non-planar structures have larger values of the lattice constant than the planar structures, and the bulk values of 10.27 au [34] is reached around $n = 9$.

3. Na adsorption on Si clusters

Four possible chemisorption sites were investigated by placing the Na adatom at different

Table 1. Ground states and energies (in au) for Si_n FCC(111) clusters.

| Cluster	Geometry	Symmetry	Ground state	a_{min} (au)	UHF energy (au)	MP4 energy (au)	MBPT binding energy per atom (eV)
$Si_2(2,0)$	linear	$D_{\infty h}$	$^3\Sigma_g$	6.1	-7.3798	-7.4598	0.98
$Si_3(3,0)$	triangle	C_{2v}	$^3B_2$	6.3	-11.0897	-11.2553	1.57
$Si_4(4,0)$	rhombus	D_{2h}	^1A_g	6.3	-14.8389	-15.0699	2.00
$Si_4(3,1)$	tetrahedron	C_s	$^1A'$	9.8	-14.7490	-14.9866	1.43
$Si_5(5,0)$	rectangle	D_{2h}	$^3B_{3u}$	6.4	-18.5152	-18.7936	1.76
$Si_5(5,0)$	trapezium	C_{2v}	$^1A'$	6.4	-18.5151	-18.8325	1.97
$Si_6(6,0)$	equilateral	C_{2v}	$^3B_2$	6.5	-22.2720	-22.6021	1.99
$Si_6(6,0)$	parallelogram	C_{2v}	$^1A'$	6.4	-22.2379	-22.6123	2.03
$Si_6(3,3)$	ring	C_s	$^1A'$	10.1	-22.1724	-22.6197	2.07
$Si_6(3,3)$	triangular prism	C_{2v}	$^1A_1$	9.5	-22.1161	-22.4726	1.40
$Si_7(1,3,3)$	capped prism	C_s	$^1A'$	10.0	-25.8257	-26.2757	1.62
$Si_7(7,0)$	hexagon	D_{2h}	$^3B_{3g}$	6.5	-25.9084	-26.3869	2.05
$Si_7(6,1)$	capped triangle	C_s	$^3A_1$	9.6	-25.8272	-26.0982	0.93
$Si_8(8,0)$	parallelepiped	C_s	$^1A'$	6.0	-29.5655	-30.1016	1.87
$Si_8(8,0)$	rectangle	D_{2h}	^1A_g	6.4	-29.6798	-30.1765	2.12
$Si_8(4,4)$	rhombic prism	C_{2v}	$^1A_1$	6.4	-29.6772	-30.1446	2.01
$Si_8(5,3)$	trapezium	C_s	$^1A'$	9.9	-29.5713	-30.0464	1.68
$Si_8(3,1,1,3)$	staggered prism	C_s	$^1A'$	10.7	-29.4521	-29.9836	1.47
$Si_9(3,3,3)$	staggered prism	C_s	$^1A_1$	10.4	-33.2681	-33.8369	1.79
$Si_9(6,3)$	antiprism	C_s	$^1A_1$	8.9	-32.9354	-33.7360	1.48
$Si_9(6,3)$	tricapped triangle	C_s	$^1A_1$	10.1	-33.3603	-33.8394	1.79
$Si_9(6,3)$	parallelepiped	C_1	$^3A'$	10.2	-33.3888	-33.7605	1.56
$Si_{10}(7,3)$	tricapped hexagon	C_s	$^1A_1$	9.9	-36.9704	-37.6486	1.93
$Si_{10}(1,3,6)$	capped antiprism	C_s	$^1A'$	9.0	-36.6621	-37.4180	1.30
$Si_{10}(3,3,3,1)$	capped staggered prism	C_1	$^1A'$	10.7	-37.0268	-37.6485	1.93
$Si_{10}(5,5)$	trapezoidal parallelepiped	C_s	$^3A'$	11.0	-37.0495	-37.5805	1.74
$Si_{10}(5,5)$	rectangular parallelepiped	D_{2h}	^1A_g	9.5	-36.8166	-37.4518	1.39
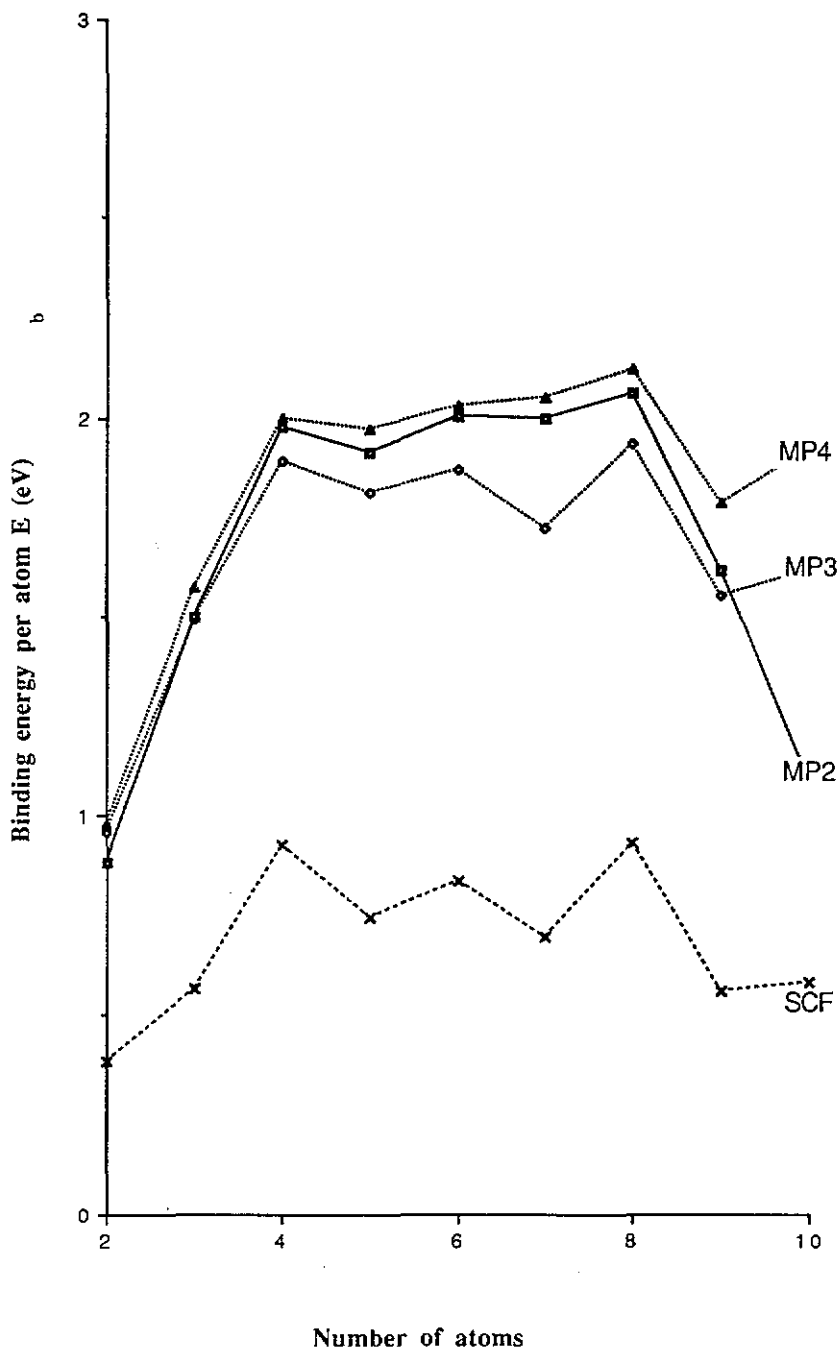
Figure 2. Binding energy (eV) versus number of atoms for $Si_n(111)$ clusters.

approach positions above the surface layer Si atoms of the twenty-six optimized clusters. The sites considered (figure 3) are the OTS, the THS, the TFS and the valley site. In the OTS, the Na atom is on top of one of the surface Si atoms. In the THS, the adatom sits at the centre of a triangle formed by the Si surface atoms whereas in the case of the TFS, the
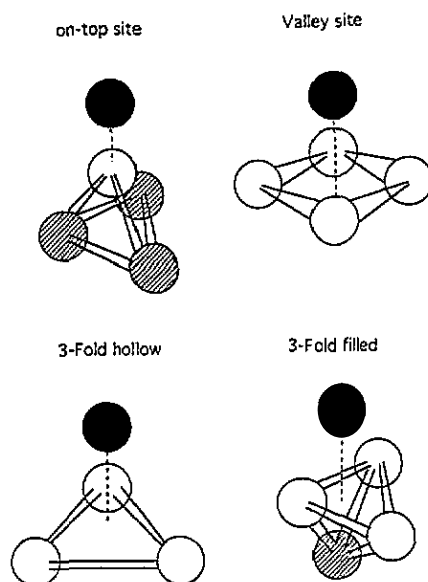
Figure 3. Adsorption sites on the ideal Si(111) surface.

adatom sits at the centre of a triangle formed by the Si surface atoms followed by another Si atom directly below it. In the valley site the adatom sits at the centre of a rhombus. The distance R of the adsorbate from the closest plane of the Si_n cluster is optimized at the UHF level of theory by considering the total energy of the AM–Si_n system as a function of the adsorbate distance R for each of the cluster systems. The value of R was allowed to become negative, the negative values corresponding to the penetration of the adsorbate atom inside the cluster. Substrate relaxation due to the adatom was not considered. The optimum geometry was then used to calculate the fourth-order perturbation-theory energy eigenvalues. To determine the relative stabilities of chemisorption at the different sites, the chemisorption energies E_c are calculated from

$$E_c = E(\text{AM}) + E\left(\text{Si}_n\right) - E\left(\text{AM–Si}_n\right) \tag{2}$$

and the results are shown in table 2. First we note that in contrast to the results for the bare clusters, the chemisorption energies at the UHF level are usually greater than those at the MP4 level. From figure 4, it is seen that in the case of the THS there is a general trend of increase in chemisorption energy with the increase of number of atoms at the MP4 level. The dip at $n = 9$ corresponds to a comparatively low value of cluster binding energy. In threefold-filled and on-top approaches we found a general reversed trend. The valley-site approach is found to be fairly independent of the cluster size. In general, we find that the presence of more atoms in the first plane decrease the chemisorption energy for all four adsorbate sites. The THS is predicted to be energetically more favourable, followed by the threefold filled, valley and on-top approaches.

To analyse the chemisorption results, we first discuss them by categories of approach positions. For the on-top position, there is a general decreasing trend in chemisorption energy with increasing n. Correlation effects are very important in this approach and change the binding energy by 275.8% and −97.4% in two of the most extreme cases. Obviously, for this position, the increased electronic repulsion plays a strong role. The MBPT chemisorption

Table 2. Total energies and chemisorption energies of Na-Si$_n$(111) systems.

System	R_{min} (au)	UHF ground-state energy (au)	MP4 ground-state energy (au)	UHF chemisorption energy E_c (eV)	MBPT chemisorption energy E_c (eV)
Adsorption on OTS					
Na-Si$_4$(1,3)	5.40	−14.9622	−15.1878	0.88	0.56
Na-Si$_5$(5,0)	5.50	−18.7605	−19.0320	1.75	1.57
Na-Si$_7$(7,0)	7.10	−26.1111	−26.586	0.60	0.50
Na-Si$_7$(6,1)	5.70	−25.9970	−26.2976	−0.29	0.51
Na-Si$_7$(1,3,3)	5.60	−26.0953	−26.4547	2.42	−0.04
Na-Si$_{10}$(7,3)	6.10	−37.2295	−37.8344	2.13	0.14
Na-Si$_{10}$(1,3,6)	5.90	−37.0228	−37.5521	4.89	−1.26
Na-Si$_{10}$(3,3,3,1)	5.45	−37.3082	−37.9018	2.74	0.07
Adsorption on valley site					
Na-Si$_4$(4,0)	5.60	−15.0605	−15.2877	1.11	1.01
Na-Si$_8$(8,0)	4.60	−29.8780	−30.3641	0.48	0.19
Na-Si$_8$(4,4)	−5.80	−29.9009	−30.3631	1.10	1.03
Adsorption on THS					
Na-Si$_3$(3,0)	5.60	−11.3160	−11.4816	1.24	1.77
Na-Si$_6$(6,0)	5.55	−22.4912	−22.8336	1.05	1.38
Na-Si$_6$(3,3)	−4.55	−22.4852	−22.8286	3.59	1.09
Na-Si$_6$(3,3)	−4.45	−22.3809	−22.7336	2.29	2.19
Na-Si$_9$(3,3,3)	8.50	−33.5287	−34.0044	2.17	−0.36
Na-Si$_9$(6,3)	−5.40	−33.1401	−33.9686	0.66	1.41
Na-Si$_9$(6,3)	4.65	−33.2994	−33.8044	4.98	−3.05
Na-Si$_9$(6,3)	−4.60	−33.6343	−34.0410	2.54	0.57
Na-Si$_{10}$(1,3,6)	−4.8	−37.0489	−37.5436	5.60	−1.49
Na-Si$_{10}$(3,3,3,1)	4.9	−37.2904	−37.9290	2.25	2.72
Adsorption on TFS					
Na-Si$_4$(3,1)	−4.80	−14.9705	−15.2248	1.11	1.57
Na-Si$_7$(6,1)	−4.80	−26.0407	−26.3054	0.89	0.72
Na-Si$_7$(1,3,3)	7.60	−26.0712	−26.5027	1.76	1.26
Na-Si$_8$(3,1,1,3)	−3.50	−29.6604	−30.1970	0.75	0.89
Na-Si$_{10}$(7,3)	4.90	−37.2368	−37.8518	2.33	0.61

energy is rather size dependent in this approach position, decreasing by 1.43 eV from n = 5 to n = 10. The adsorbate distance R increases by 12.9% from smaller to larger clusters. If one compares the systems Na-Si$_7$(7,0) and Na-Si$_{10}$(7,3), one notes that the presence of second-layer atoms lower the chemisorption energy and the adsorbate–cluster distance. This has been noted before in our work for hydrogen interaction with lithium clusters [35, 36]. The presence of atoms in the third layer also lowers the chemisorption energy but helps increase the adsorbate–cluster distance. This trend can be explained in terms of a strongly localized bond between the adsorbate and the substrate atom directly below it, which is weakened by the presence of Si atoms in additional layers.

For the valley site there is a comparatively large decrease in the adsorbate distance from Si$_4$(4,0) to Si$_8$(8,0). Penetration of the adatom inside the cluster is characterized by a rather small increase of 0.02 eV in chemisorption energy. Correlation effects appear to be much less significant for the valley site. In the case of the threefold hollow approach, the chemisorption energy E_c is strongly size dependent, with an increase of 0.95 eV from
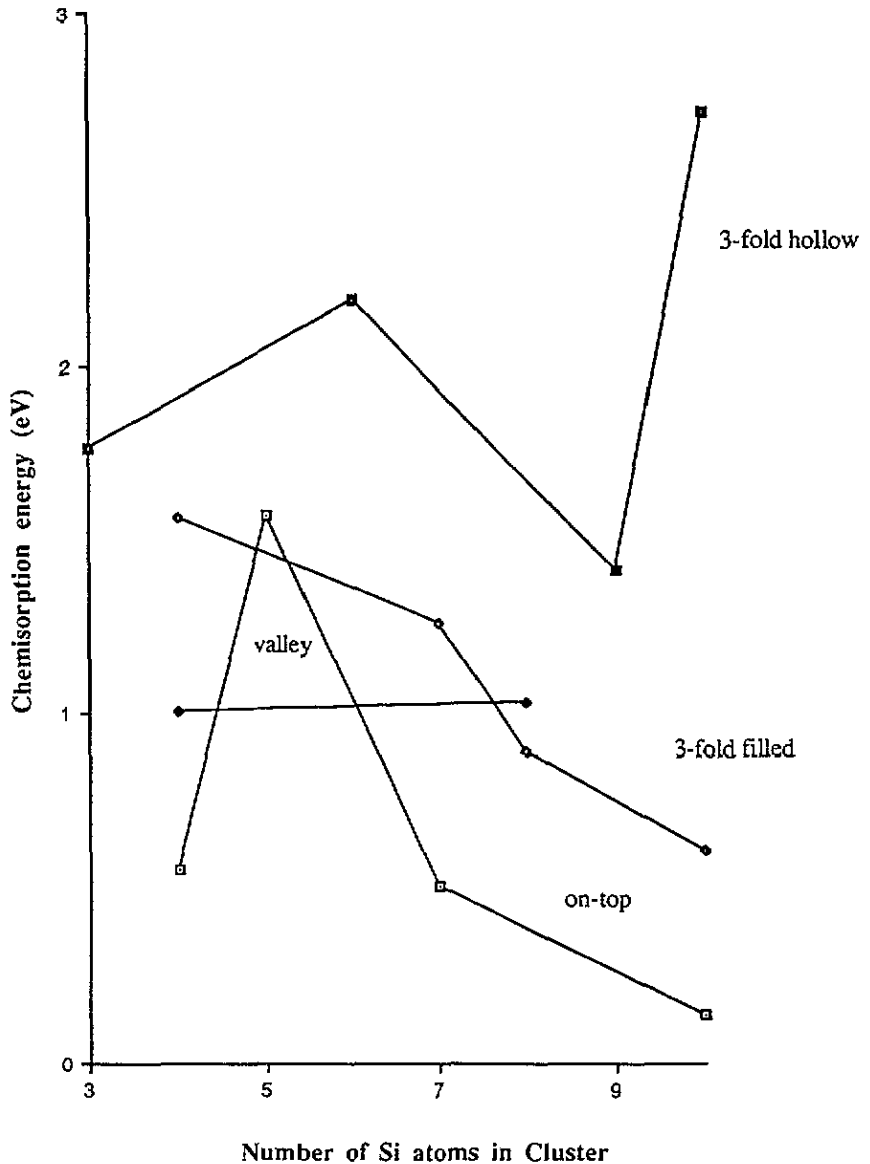
Figure 4. Chemisorption energy of an Na atom on Si clusters at different sites.

smaller to larger clusters. The chemisorption energy is also cluster geometry dependent. For example in the case of Na–Si$_6$, E_c ranges from 1.09 to 2.19 eV while for Na–Si$_9$ it ranges from 0.57 to 1.41 eV. This difference in E_c can be attributed to the difference in binding energies for the particular cluster and we find that a low chemisorption energy corresponds to a more stable cluster and vice versa [35, 36]. In this approach, the presence of second-layer atoms usually increases the chemisorption energy by penetration of the adatom inside the cluster while the presence of atoms in the third layer makes E_c negative by increasing the adsorbate distance. For the TFS approach, there is a general trend of

decrease in chemisorption energy with increasing number of atoms, decreasing by 0.96 eV from Si_4 to Si_{10}. For this adsorption position, there is a general decrease in the value of E_c as the number of layers increases, but for the systems with equal numbers of atoms as in the case of Na–Si_7, the presence of third-layer atoms increases the chemisorption energy. In this case penetration of the adatom inside the cluster is accompanied by a decrease in E_c.

4. Electron charge distributions

It is important to study the distribution of electronic charge in the AM–Si systems in view of the controversy surrounding the nature of the adsorbate–substrate bond and the possibility of the transfer of electronic charge from the AM atom to the Si surface. In the current calculations, the gross atomic populations for both the Si and AM–Si cluster systems were first obtained from Mulliken population analysis [37], where the gross atomic populations are defined in terms of the basis function populations q_m by

$$q_A = \sum_{\mu}^{A} q_m. \tag{3}$$

The atomic charge on atom A is defined to be $(Z_A - q_A)$, where Z_A is the atomic number of A. Finally the changes ΔQ in atomic charges resulting from AM adsorption on Si_n clusters are calculated using the formula

$$\Delta Q = Q(\text{AM–}Si_n) - Q(\text{AM, } Si_n). \tag{4}$$

The values of changes in electronic charge for Na adsorption are listed in table 3. The Si atoms in this table are grouped together by symmetry equivalence for the atomic populations and the number of atoms in each group is given in parentheses.

For the on-top site, the charge transfer ranges from 0.56 to 0.80 (in units of electronic charge). The charge transfer from adsorbate to substrate increases by 0.1 from the second layer Na–Si_4(1,3) to the third layer Na–Si_7(1,3,3), but the presence of atoms in the fourth layer decreases the charge transfer by approximately the same amount. If we compare Na–Si_5(5,0) and Na–Si_7(7,0), we notice that the presence of more atoms in the first layer increases the charge transfer. The presence of atoms in the second layer decreases the charge transfer, as do the atoms in the third and fourth layers. For the valley-site approach, the increase in charge transfer is significantly low (0.05) from Na–Si_4 to Na–Si_8, which might be compared with the difference in chemisorption energies of the corresponding clusters, which is only 0.02 eV. Here we find that charge transfer increases due to the presence of atoms in the second layer and, for planar clusters, more atoms in the first plane increase the charge transfer. On the other hand, the amount of charge transferred changes by 50% in the THS from smaller to larger clusters. It is found that the presence of atoms in the second and third layers of the cluster increases the charge transfer from the adsorbate while the fourth-layer atoms significantly decrease it. In the threefold-filled approach, the charge transfer ranges from 0.21 to 0.78. One notes that in case of Na–Si_8(3,1,1,3) the charge transfer is very low (0.21) due to the presence of atoms in the fourth layer. The presence of atoms in the third layer increases ΔQ while atoms in the fourth layer significantly decrease it. Analysing all four adsorbate sites, it can be concluded that in general the charge transfer increases while increasing number of atoms up to the third layer except for the on-top

Table 3. Changes ΔQ in gross atomic charges between Na–Si$_n$ and Na plus Si$_n$ in the FCC(111) symmetry.

Cluster	ΔA(Na)	ΔQ(Si)	ΔQ(Si)	ΔQ(Si)	ΔQ(Si)	ΔQ(Si)	ΔQ(Si)	ΔQ(Si)	
Adsorption position: OTS									
Na–Si$_4$(1,3)	0.66	−0.13	−0.14(2)	−0.25					
Na–Si$_5$(5,0)	0.56	−0.23	−0.08(4)						
Na–Si$_7$(7,0)	0.77	−0.30	−0.05(4)	−0.13(2)					
Na–Si$_7$(1,3,3)	0.76	−0.00	−0.08(3)	−0.04	−0.09	−0.37			
Na–Si$_7$(6,1)	0.80	0.21	0.02	0.01	−0.12(2)	−0.43	−0.39		
Na–Si$_{10}$(3,3,3,1)	0.67	−0.06(2)	−0.04(3)	−0.01	−0.03(2)	−0.00	−0.36		
Na–Si$_{10}$(7,3)	0.70	−0.27	−0.11(2)	−0.12(2)	−0.1(2)	0.08(3)			
Na–Si$_{10}$(1,3,6)	0.61	0.01	0.10(2)	−0.24(2)	−0.25	0.04	0.11(2)	−0.35	
Adsorption position: valley site									
Na–Si$_4$(4,0)	0.52	−0.27(2)	0.01(2)						
Na–Si$_8$(4,4)	0.56	−0.28	0.00(5)	−0.27					
Na–Si$_8$(8,0)	0.57	0.04(2)	−0.14(2)	−0.09(4)	0.04				
Adsorption position: THS									
Na–Si$_3$(3,0)	0.46	−0.12	−0.17(2)						
Na–Si$_6$(6,0)	0.63	−0.20	−0.11	−0.39	0.18	−0.05(2)			
Na–Si$_6$(3,3)	0.51	−0.16(3)	−0.01(3)						
Na–Si$_6$(3,3)	0.59	−0.17(2)	−0.26	0.04(2)	−0.07				
Na–Si$_9$(3,3,3)	0.71	0.09	0.07	0.12	−0.27	−0.16	−0.23	−0.1(2)	−0.12
Na–Si$_9$(6,3)	0.68	−0.16	−0.16(2)	−0.10	−0.11	−0.09	0.03(3)		
Na–Si$_9$(6,3)	0.52	0.05	0.06(2)	−0.22(2)	−0.15	−0.07	−0.01(2)		
Na–Si$_9$(6,3)	0.64	−0.13	−0.25(2)	−0.20(2)	−0.12	0.16(2)	0.21		
Na–Si$_{10}$(1,3,6)	0.69	−0.14	−0.06(2)	−0.27(2)	−0.23	0.08	0.14(2)	−0.02	
Na–Si$_{10}$(3,3,3,1)	0.54	0.00(5)	0.01	−0.18(2)	−0.15	−0.03			
Adsorption position: TFS									
Na–Si$_4$(3,1)	0.40	−0.24	−0.15(2)	0.13					
Na–Si$_7$(6,1)	0.55	−0.09	−0.32	−0.12	−0.00	0.06	−0.15	0.08	
Na–Si$_7$(1,3,3)	0.70	−0.00(3)	−0.23(3)	−0.01					
Na–Si$_8$(3,1,1,3)	0.21	−0.21	−0.17(2)	0.23	0.02	0.01	0.04(2)		
Na–Si$_{10}$(7,3)	0.78	0.11	−0.02(4)	−0.04	−0.03	−0.25(2)	−0.23		

position and atoms in the fourth layer cause a hindrance to chemisorption. Usually more atoms in the first plane increase the charge transfer significantly.

We now make some comparisons with other calculations to arrive at a picture of alkali-atom–Si(111) surface interaction. In our present work, using *ab initio* self-consistent UHF and MP4 total-energy cluster calculations with Hay–Wadt effective core potentials [38, 39], the THS is found to be the most favourable adsorption position for Na and the bonding between AM and Si substrate is observed to be neither purely ionic nor covalent but of mixed type. Partially ionic bonding was also observed in the *ab initio* molecular-dynamic (MD) study of Moullet *et al* [40, 41] for the Si(111):Na system. In this MD simulation, the basic geometry consisted of one layer of Na and eight layers of Si. The valence electrons were treated in the local-density approximation (LDA) of the density-functional theory and the core–valence interaction was described by angular-momentum-dependent pseudopotentials. In our calculations, the Si–Na distances are found to be 6.16 au, 6.23 au, 6.02 au and 5.4 au for the THS, TFS, valley site and OTS respectively. For the most favourable adsorption site (THS), our predicted value is 0.55 au larger than the calculated value of Moullet *et al*

[40,41], whereas for the TFS and OTS, the values are respectively 0.4 au and 0.1 au larger. The difference in the methodologies might be the cause of these discrepancies. Northrup's [8] LDA calculations using self-consistent pseudopotentials also favoured the THS, but the bonding was found to be ionic. From the results of angle-resolved inverse and ultraviolet (direct) photoemission spectroscopy (IPS and UPS respectively) studies, Reihl *et al* [42] found the THS to be the most favoured site, but the bonding was ionic. As far as charge transfer is concerned, it is observed in our calculations that the charge transfer is not confined to the first Si layer only as indicted from the MD simulation calculation [40,41], but the charge transferred from the Na atom to the substrate, which is consistent with the experimental observation of Reihl *et al* [42]. The decrease in the HOMO–LUMO gap in our calculations also indicated the possibility of metallization.

Acknowledgments

References

[1] Ernst J H and Yu M L 1990 *Phys. Rev.* B **41** 12953
[2] Laubshat C, Prietsch M, Domke M, Weschke E, Mandel T, Remmers G, Ortega J E, Xue C and Kaindl G 1989 *Metallization and Metal–Semiconductor Interfaces (NATO ASI Ser B)* vol 195, ed I P Batra (New York: Plenum)
[3] Monch W 1989 *Metallization and Metal–Semiconductor Interfaces (NATO ASI Ser B)* vol 195, ed I P Batra (New York: Plenum)
[4] Batra I P and Bagus P S 1988 *J. Vac. Sci. Technol.* A **6** 600
[5] Redondo A, Goddard W and McGill T C 1982 *J. Vac. Sci. Technol.* **21** 649
[6] Avci R 1986 *J. Vac. Sci. Technol.* A **4** 1400
[7] Papageorgopoulos C and Kamaratos M 1992 *J. Phys.: Condens. Matter* **4** 1935
[8] Northrup J E 1986 *J. Vac. Sci. Technol.* A **4** 1404
[9] Ossicini S, Arcangeli C and Bisi O 1990 *Phys. Rev.* B **42** 7671
[10] Batra I P and Ciraci S 1988 *Phys. Rev.* B **37** 8432
[11] Ekpenuma S N and Ray A K 1992 *Phys. Rev.* B **46** 16163
[12] Ekpenuma S N and Ray A K 1991 *Surf. Sci. Lett.* **257** L659
[13] Ekpenuma S N and Ray A K 1992 *J. Phys.: Condens. Matter* **4** 5077
[14] Szabo A and Ostlund N S 1982 *Modern Quantum Chemistry* (New York: Macmillan)
[15] Hehre W J, Radom L, Schleyer P V R and Pople J A 1986 *Ab Initio Molecular Orbital Theory* (New York: Wiley–Interscience)
[16] Goldstone J 1957 *Proc. R. Soc.* A **239** 267
[17] Lowdin P O 1965 *J. Math. Phys.* **6** 1341
[18] Lowdin P O 1965 *Phys. Rev.* **139** A357
[19] Hira A S and Ray A K 1991 *Surf. Sci.* **249** 199
[20] Elbert S T and Lam B 1987 *Quantum Chem. Program Exchange Bull.* **7** 115
[21] Frisch M J, Trucks G W, Head-Gordon M, Gill P M W, Wong M W, Foresman J B, Johnson B G, Schlegel H B, Robb M A, Replogle E S, Gomperts R, Andres J L, Raghavachari K, Binkley J S, Gonzalez C, Martin R L, Fox D J, Defrees D J, Baker J, Stewart J J P and Pople J A 1992 *GAUSSIAN 92* Revision C (Pittsburgh, PA: Gaussian Inc)
[22] Moore C E 1969 *Atomic Energy Levels (National Standard Reference Data Service National Bureau of Standards Circulation No 35)* (Washington, DC: US GPO)
[23] Raghavachari K 1986 *J. Chem. Phys.* **84** 5672

[24] Raghavachari K and Rohlfing C M 1988 *J. Chem. Phys.* **89** 2219

[25] Rohlfing C M Raghavachari K 1990 *Chem. Phys. Lett.* **167** 559

[26] Bloomfield L A, Freeman R R and Brown W L 1985 *Phys. Rev. Lett.* **54** 2246

[27] Bloomfield L A, Geusic M E, Freeman R R and Brown W L 1985 *Chem. Phys. Lett.* **121** 33

[28] Heath J R, Liu Y, O'Brien S C, Zhang Q L, Curl R F, Tittel F K and Smalley R E 1985 *J. Chem. Phys.* **83** 5520

[29] Liu Y, Zhang Q L, Tittel F K, Curl R F and Smalley R E 1986 *J. Chem. Phys.* **85** 7434

[30] Martin T P and Schaber H 1985 *J. Chem. Phys.* **83** 855

[31] Huber K P and Herzberg G 1979 *Constants of Diatomic Molecules* (New York: Van Nostrand Reinhold)

[32] Cuthbertson A F and Glidewell C 1981 *Inorg. Chim. Acta* **49** 91

[33] Martin T P and Schaber H 1979 *Z. Phys.* B **35** 61

[34] American Institute of Physics 1979 *American Institute of Physics Handbook* 3rd edn (New York: McGraw-Hill)

[35] Ray A K and Hira A S 1988 *Phys. Rev.* B **37** 9943

[36] Hira A S and Ray A K 1989 *Phys. Rev.* B **40** 3507

[37] Mulliken R S 1955 *J. Chem. Phys.* **23** 1841

[38] Hay P J and Wadt W R 1984 *J. Chem. Phys.* **82** 284

[39] Wadt W R and Hay P J 1985 *J. Chem. Phys.* **82** 299

[40] Moullet I, Andreoni W and Parrinello M 1992 *Phys. Rev.* B **46** 1842

[41] Moullet I, Andreoni W and Parrinello M 1992 *Surf. Sci.* **269** 1000

[42] Reihl B, Sorensen S L, Dudde R and Magnusson K O 1992 *Phys. Rev.* B **46** 1838